ISSN 1027-5495. Functional Materials, 28, No.4 (2021), p. 694-700.
doi:https://doi.org/10.15407/fm28.04.694 © 2021 — STC "Institute for Single Crystals"

Research of properties of AlB_{12}–Al electric spark coatings on VT1-0 titanium alloy

A.P.Umanskyi[1], M.S.Storozhenko[1], V.E.Sheludko[1], V.B.Muratov[1], V.V.Kremenitsky[2], I.S.Martsenyuk[1], M.A.Vasilkovskaya[1], A.D.Kostenko[1], A.A.Vasiliev[1], A.E.Terentiev[1]

[1]I.Frantsevich Institute for Problems of Materials Science, National Academy of Sciences of Ukraine, 3 Krzhyzhanovsky Str., 03142 Kyiv, Ukraine
[2]Technical Center, National Academy of Sciences of Ukraine, 13 Pokrovskaya Str., 04070 Kyiv, Ukraine

Received February 11, 2021

The article investigates the kinetics of mass transfer of the electrode material AlB_{12}-50 wt.% Al during electrospark alloying (ESA) of the titanium alloy VT1-0, as well as the structure and properties of the resulting coating. The coating was applied using an ALIER-52 installation. The thickness (340 μm), microhardness (4–8 GPa) and wear rate were determined. The coating is multiphase: Ti aluminide, Ti and Al oxides, Ti and TiB_2 are found. The wear of the ESA-coated specimens is shown to be much less than that of the uncoated one. A conclusion is made about the possibility of using this electrode material for ESA process.

Keywords: AlB_{12}–Al, ESA, mass transfer kinetics, structure, phase composition, microhardness, wear rate.

Дослідження властивостей електроіскрових покриттів AlB_{12}–Al на титановому сплаві ВТ1-0. *О.П.Уманський, М.С.Стороженко, В.Є.Шелудько, В.Б.Муратов, В.В.Кременицький, І.С.Марценюк, М.А.Васильківська, О.Д.Костенко, О.О.Васільєв, О.Є.Терентьєв*

Досліджено кінетику масообміну електродного матеріалу AlB_{12}-50 мас.% Al при електроіскровому легуванні (ЕІЛ) титанового сплаву ВТ1-0, а також структуру та властивості отриманого покриття, що нанесене на установці ALIER-52. Для нього визначено товщину (340 мкм), мікротвердість (4–8 ГПа) та інтенсивність зношування. Покриття багатофазне, визначено алюмінід Ti, оксиди Ti та Al, титан та TiB_2. Показано, що знос зразку з ЕІ-покриттям значно менший, ніж зразку без покриття. Зроблено висновок про перспективність застосування даного електродного матеріалу для ЕІЛ.

Исследованы кинетика массопереноса электродного материала AlB_{12}-50 масс.% Al при электроискровом легировании (ЭИЛ) титанового сплава ВТ1-0, а также структура и свойства полученного покрытия, нанесенного на установке ALIER-52. Для него определены толщина (340 мкм), микротвёрдость (4–8 ГПа) и интенсивность изнашивания. Покрытие многофазное, отмечены алюминид Ti, оксиды Ti и Al, титан и TiB_2. Показано, что износ образца с ЭИ-покрытием значительно меньше, чем образца без покрытия. Сделан вывод о перспективности применения данного электродного материала для ЭИЛ.

1. Introduction

Among the wide range of constructional materials, the titanium alloys occupy a special place, the most important advantages of which are high strength and high temperature resistance in combination with high corrosion resistance. Due to low density, good weldability, resistance to erosion and cavitation, the titanium alloys are widely used in aircraft industry, rocket science, shipbuilding, as well as in chemical engineering, food engineering, transport engineering and medicine [1–3]. For example, in the PS-90A aircraft engine for the Ilyushin Il-96, Ilyushin Il-76, and Tupolev Tu-204 planes, 10 % of the parts are made of various titanium alloys, and in the designs of planes of the AN family (ANTONOV company) the mass of such parts is 8–9 % of the mass of the airframe [4, 5].

However, the titanium alloys are characterized by low hardness, wear resistance and scuffing resistance. Therefore, in order to extend the working life of the parts made of the titanium alloys, various types of processing are used, such as mechanical, thermal, chemical-thermal, and also protective coatings are applied (diffusion, ion-plasma, detonation, electric spark [6–11]).

During electrospark alloying (ESA), the electrode material (anode) is transferred to the surface of the part (cathode) to form a hardened layer with improved physical and mechanical properties. Various refractory compounds, namely carbides, nitrides, aluminides, silicides and borides, can be used as the anode material [12–14]. Among the latter, aluminum dodecaboride AlB_{12} is of interest. The method of its synthesis from Al and BN, developed at the Frantsevich Institute for Materials Science Problems of NAS of Ukraine, turned out to be more rational and cost-effective than direct synthesis from Al and B [15]. AlB_{12} has a low density (~2.52 g/cm^3), and the peculiarity of its crystal structure (icosahedral boron framework) determines its high hardness (22–24 GPa) and infusibility (2070°C) [16].

However, the low crack resistance of aluminum dodecaboride significantly limits the scope of its application [16]; therefore, it is advisable to use AlB_{12} in combination with ductile bonded metal. It is promising to use aluminum, which is characterized by high plasticity, low density (2.7 g/cm^3) and low melting point (660°C). Earlier it was found that Al wets AlB_{12} well with the formation of contact angles (≈20 deg), and there are no secondary phases in the interaction zone at the Al–AlB_{12} interface [16]. In addition, aluminum has a resistivity of 2.7 $\mu\Omega \cdot$ cm, which is 60 % less than that of copper; thereby it acts as a kind of additive increasing the conductivity of the AlB_{12}–Al composite (a resistivity of AlB_{12} — 10^6 Ω·cm), which is of great importance in ESA.

So, the aim of the work is to investigate the possibility of using the composite material "AlB_{12}–Al" to obtain ESA-coatings on titanium alloys, and to study the properties of these coatings.

2. Experimental

AlB_{12} samples were prepared from a powder synthesized at the IPMS of NASU according to the procedure described in [17, 18]. AlB_{12} with a porous ceramic framework was obtained. Then it was impregnated with an Al melt in vacuum ($1.33 \cdot 10^{-4}$ Pa) at a temperature of ~1100°C. This made it possible to obtain a composite material aluminum matrix AlB_{12}–50 wt.% Al in the form of a bar of 50×50×5 mm in size, from which electrodes for ESA were cut by the electroerosive method.

Fig. 1 shows the microstructures of the electrode material AlB_{12}-50 wt.% Al, obtained on a JEOL JAMP9500F microanalyzer. The material consists of three phases: a metal matrix, AlB_{12} grains (the size of which varies in the range of 1–4 μm) uniformly distributed in the matrix, and Al_2O_3

Table 1. Chemical composition of the composite material AlB_{12}-50 wt.% Al

Spectrum	Element, wt.%						Total
	B	C	N	O	Al	Fe	
1	82.07	0.66	–	0.03	16.92	0.32	100.00
2	81.52	0.88	0.15	0.05	17.00	0.40	100.00
3	78.77	3.94	1.01	0.45	15.83	–	100.00
4	0.26	0.60	0.67	47.02	51.45	–	100.00
5	1.37	1.97	0.11	1.81	94.74	–	100.00

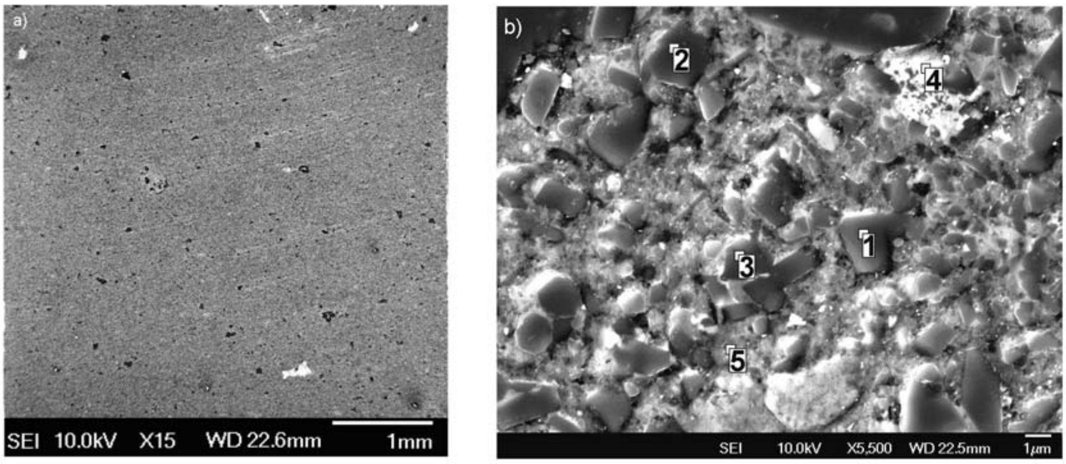

Fig. 1. Microstructure of the electrode material AlB_{12}-50 wt.% Al: a) — general view; b) — enlarged fragment with elemental analysis data.

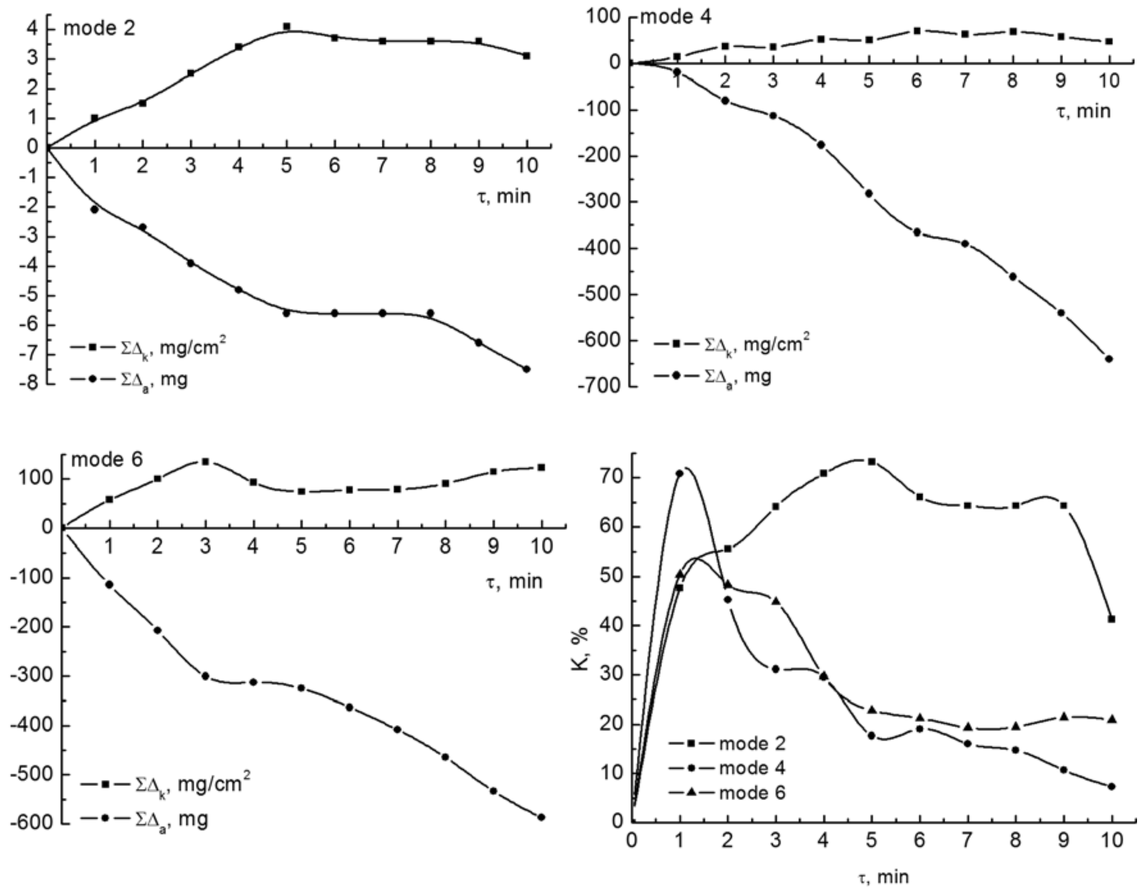

Fig.2. Kinetic dependences of the total gain in the cathode mass , the total erosion of the anode , the average value of the mass transfer coefficient at ESA of 1cm^2 of the VT1-0 alloy.

particles (Fig. 1b). The chemical composition of the main phases of the composite AlB_{12}-50 wt.% Al was determined by micro X-ray spectral analysis (Table 1).

Electrospark alloying of the samples of the titanium alloy VT1-0 (GOST 19807-91) of 11.3 mm in a diameter was carried out on an ALIER-52 installation (SCINTI, Chisinau,

Table 2. Technological parameters of the ALIER-52 installation

Mode	Pulse duration, μs±20 %	Pulse current amplitude value, A±20 %	Pulse energy, E, J
2	40	125	0.09
4	170	200	0.61
6	700	200	2.52

RM) at the modes indicated in Table 2. For each minute of processing of 1 cm^2 of the sample surface, the specific erosion of the anode (Δa) and specific gain in the cathode mass (Δk) were measured with an accuracy of 10^{-4} g on an electronic balance OHAUS Adventurer AR0640. The total anode erosion ($\sum\Delta a$) and gain in the cathode mass ($\sum\Delta k$), as well as the average mass transfer coeffi-

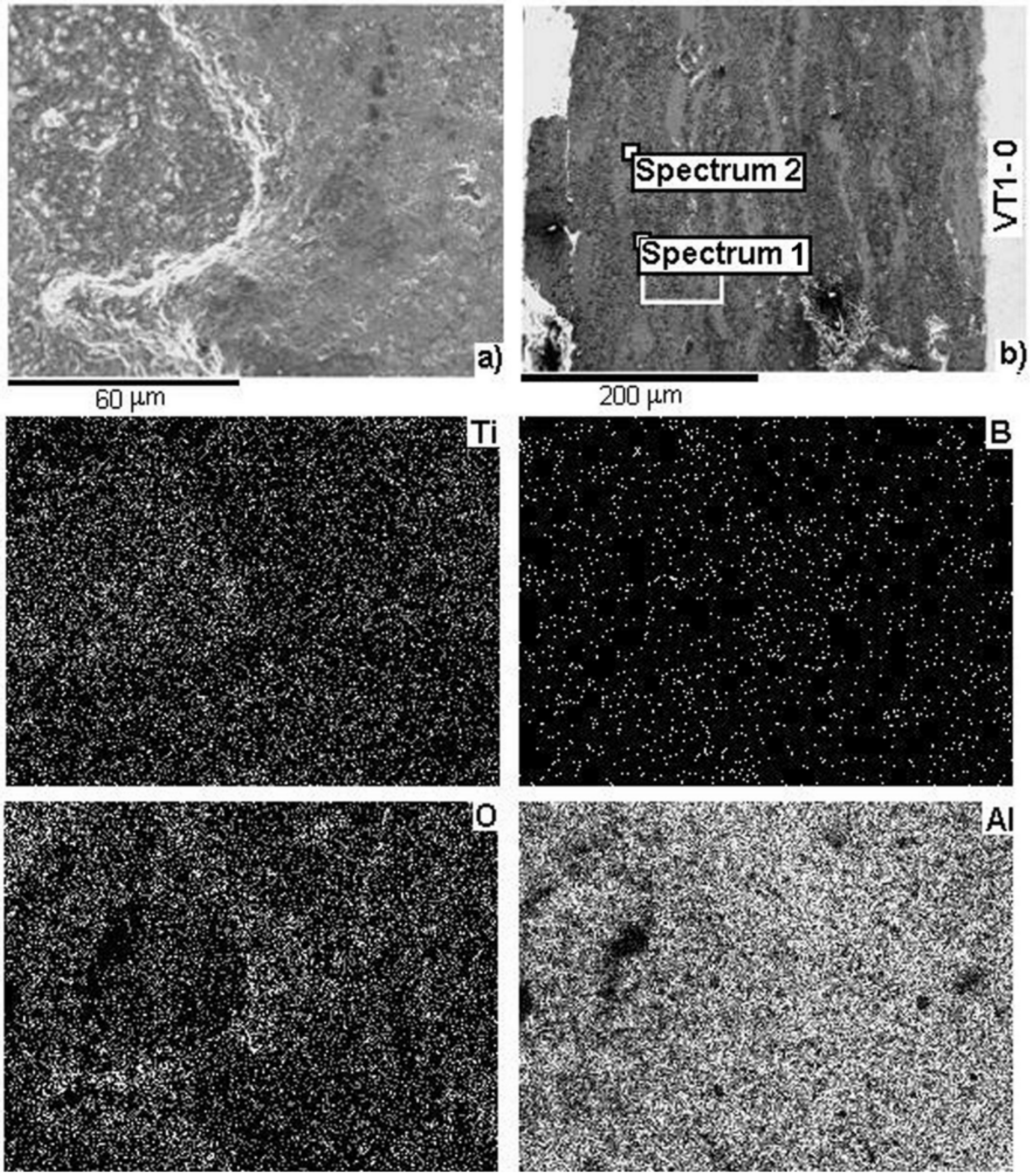

Fig. 3. Microstructure of the AlB_{12}–50 wt.% Al ES-coating of on the VT1-0 alloy: a) — coating surface in X-ray radiation with distribution of the elements over its surface, b) — cross-section of the coating with elemental analysis.

Table 3. Physical characteristics of the electrode materials and the value of the Palatnik criterion

Characteristic	Anode (AlB_{12}-50 wt.% Al)	Cathode (VT1-0) [22]	The value of the Palatnik criterion τ_a/τ_c
λ, W/(m·K)	72.58	18.85	0.57
C_p, J/(kg·K)	918.88	540	
T_m, K	933*	1941	
ρ, kg/m^3	2616	4505	

* T_m of the most low-melting phase (Al) was used for the calculation

Table 4. Elemental analysis of the cross-section of the ES-coating (Fig. 3b)

Spectrum	Element, wt.%				Total
	B	N	O	Al	
1	44.28	–	3.41	52.31	100.00
2	56.12	5.84	1.57	36.46	100.00

cient $K' = \sum\Delta k/\sum\Delta a$ were calculated during the alloying time $\tau = 10$ min/cm^2.

The density of the electrode material was determined by the method of hydrostatic weighing (GOST 25281-82). Heat capacity was measured using the calorimetric method (GOST 23250-78). Thermal conductivity coefficient was obtained according to the method described in [19]. The microhardness of the coatings was measured on a PMT-3 microhardness tester at a load of P = 0.5 H. Tribotechnical studies of the coatings were carried out on a MT-68 installation according to the pin-on-disk scheme in the mode: P = 0.2 MPa, V = 4 m/s, friction path S = 3 km. Hardened U8 steel (HRC 61-63) was used as a counterbody.

X-ray analysis of the friction surface was carried out on a DRON-3M diffractometer in CuK_α filtered radiation. The structure of the coatings was studied using a JEOL JSM-6490 LV scanning electron microscope equipped with systems of energy-dispersive X-ray microanalysis and reflected electron diffraction.

3. Results and discussion

It is possible to theoretically evaluate the interaction between the electrode and the substrate and to some extent predict the composition of the coating using the Palatnik criterion [20, 21] which connects only physical constants of electrode materials as follows:

$$\frac{\tau_a}{\tau_c} \cong \frac{c_a\rho_a\lambda_a(T_a - T_0)^2}{c_c\rho_c\lambda_c(T_c - T_0)^2},$$

where τ_a and τ_c are the characteristic times of erosion (formation of melting centers in the discharge zone) of the anode and the cathode, respectively; $C_{a,c}$ is the heat capacity, J/(kg·K); $\rho_{a,c}$ is the density, kg/m^3; $\lambda_{a,c}$ is the coefficient of thermal conductivity, W/(mK); $T_{a,c}$ is the melting point, K; T_0 is the ambient temperature.

This ratio does not take into account a large number of factors affecting the ESA process, but, it can be used for a quantitative evaluation of 3 types of interactions between anode and cathode made of different materials, namely:

— at $\tau_a << \tau_c$ a coating is formed on a cathode surface;

— at $\tau_a \sim \tau_c$ it is possible to form a coating in the form of an anode-cathode alloy;

— at $\tau_a >> \tau_c$ there is no material transfer from the anode to the cathode, but the transfer of material from the cathode to the anode is possible [20, 21].

The data required for calculations according to the Palatnik criterion in our conditions are given in Table 3. It follows from the calculations that it is possible to obtain an ES coating from AlB_{12}-50 wt% Al on a VT1-0 substrate.

Fig. 2 shows the kinetic dependences of the total anode erosion and the cathode mass gain. These data indicate that at a pulse energy of E = 0.09 J (mode 2), for 5 min of alloying we obtain $\sum\Delta k$ = 4.1 mg/cm^2 and $\sum\Delta a$ = 5.6 mg. After 10 min, $\sum\Delta k$ decreases to 3.1, and $\sum\Delta a$ increases to 7.5 mg, respectively. After 5 min, the average coefficient of mass transfer K' is 73.21 %. The negative cathode mass gain was recorded for the first time after 6 min (i.e., the threshold of the brittle destruction of the doped layer is T_x = 6).

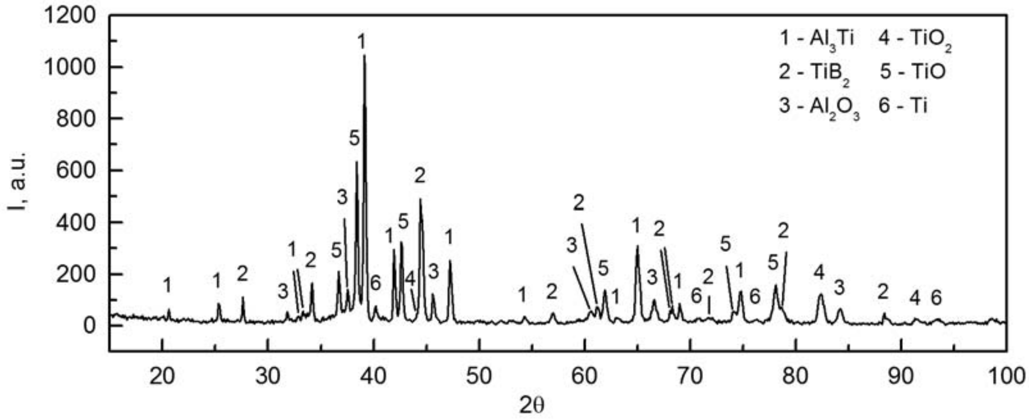

Fig. 4. Diffraction pattern of the ES-coating AlB_{12}-50 wt.% Al on the VT1-0 alloy.

With an increase in the pulse energy to $E = 0.61$ J (4 mode), $\sum \Delta k = 36.2$ mg/cm^2, $\sum \Delta a = 80$ mg for 2 min of alloying. Under these conditions, K' is 70.83 % for 1 min of treatment with a decrease to 45.25 % after 2 min: $T_x = 3$.

6 mode ($E = 2.52$ J) is characterized by the values of $\sum\Delta k = 134.8$ mg/cm^2 and $\sum\Delta a = 300$ mg for 3 min of treatment. $K' =$ 50.43 % for 1 min, followed by a decrease to 44.87 % for 3 min, $T_x = 4$.

The modes 4 and 6 are characterized by a rather high values of $\sum \Delta k$ and K' in the first minutes of alloying. To choose the most effective mode, we use the efficiency criterion for the formation of the doped layer γ_{DL} [23]:

$$\gamma_{DL} = \Delta_c \cdot K_{av}' \cdot T_x,$$

where Δ_c is the cathode mass gain, g/cm^2; K_{av} is the average mass transfer coefficient during T_x; T_x is the specific time up to the beginning of the Al brittle destruction, min/cm^2.

Calculations have shown that $\gamma_{DL} = 3.93$ and 6.64 (g·min)/cm^4 for modes 4 and 6, respectively, i.e. the efficiency of the ESA process increases with pulse energy increasing, which correlates with [23]. So, the ESA process in mode 6 is more efficient, and the coating applied in it was chosen for further research.

The microstructure of the surface of the ES-coating and its cross-section with an elemental analysis at the separate points (Table 4) are shown in Fig. 3. These data indicate that the coating surface in mode 6 is melted and homogeneous in structure. Al, O, Ti and B elements are evenly distributed.

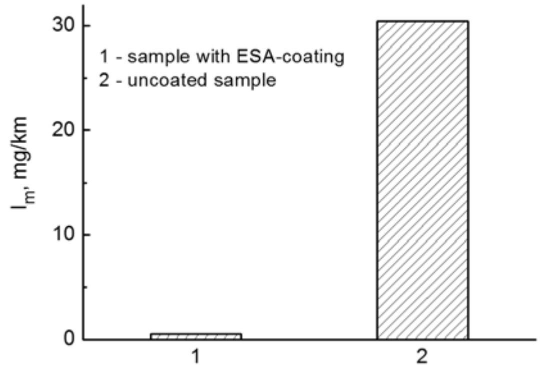

Fig. 5. Wear rate of the ES-coating AlB_{12}-50 wt.% on the VT1-0 alloy (mode 6).

X-ray analysis (Fig. 4) showed the phases of titanium, titanium aluminide (Al_3Ti), titanium and aluminum oxides, and titanium diboride in the coating. The formation of the Al_3Ti phase was observed during ESA of the VT1 alloy using an aluminum electrode [10]. The absence of the AlB_{12} phase is noteworthy. The ESA process occurring at plasma temperatures (2·10^4 K) in air is known to be accompanied by thermo-oxidative destruction of anode and cathode materials [24]. Such harsh conditions lead to the destruction of aluminum dodecaboride into its constituent elements at $T = 2300$ K [25].

The thickness of the coating is 340 μm (Fig. 3b). The microhardness H_μ varies from 4 to 6–8 GPa. It can be explained by the presence of the TiB_2 phase, titanium aluminide Al_3Ti, and Al_2O_3 (hardness 12–14 GPa). The data correlate with similar ones given in [11].

The wear rate I_m of the sample with ES-coating applied in mode 6 is much less than that for the uncoated one (Fig. 5). Such an increase in wear resistance can be explained by the presence of Al_3Ti, TiB_2, and Al_2O_3 — materials known for their wear resistance and hardness [26–30] in the ESA coating. The friction coefficient is $f = 0.36$.

4. Conclusions

The process of the formation of AlB_{12}-50 wt.% Al ES-coatings on the titanium alloy VT1-0 has been studied. Based on the analysis of the kinetic dependences of mass transfer as well as on the calculated efficiency criterion for the formation of the alloyed layer γ_{DL}, the processing mode 6 (E = 2.52 J) was determined as optimal. This is characterized by rather high values of the total cathode mass gain and mass transfer coefficient in the first minutes of alloying.

The obtained ES-coating has a thickness of 340 μm and microhardness from 4 to 6–8 GPa. ES treatment increases the wear resistance of the titanium alloy due to the formation of Al_3Ti, TiB_2 and Al_2O_3 in the coating structure.

The AlB_{12}–Al system is promising from the point of view of its possible application for ESA coating.

References

1. B.A.Kolachev, V.I.Elagin, V.A.Livanov, Metal Science and Heat Treatment of Non-ferrous Metals and Alloys, MISIS, Moscow (1999) [in Russian].
2. I.V.Gorynin, S.S.Ushakov, A.N.Khatuntsev et al., Titanium Alloys for Marine Engineering, Polytekhnika, St. Petersburg (2007) [in Russian].
3. Titanium and Titanium Alloys: Fundamentals and Applications, ed. by C.Leyens, M.Peters, Wiley-VCH Verlag GmbH & Co. KgaA, Weinheim (2003).
4. Yu.P.Reshetnikov, *Titan*, **1–2**, 9 (1995).
5. S.L.Antonyuk, A.G.Molyar, A.N.Kalinyuk et al., *Adv. Electrometallurgy*, **1**, 9 (2003).
6. ASM Handbook Volume 4E: Heat Treating of Nonferrous Alloys, ed. by G.E.Totten, Materials Park, Ohio, USA: ASM International (2016).
7. Lai-Chang Zhang, Liang-Yu Chen, Liqiang Wang, *Adv. Eng. Mater.*, **22**, 1901258 (2020). https://doi.org/10.1002/adem.201901258.
8. S.N.Bratushka, L.V.Malikov, *VANT*, **6**, 126 (2011).
9. S.Panin, V.Vlasov, D.Dudina, *Metals*, **7**, 355 (2017). htpss://doi.org/10.3390/met7090355.
10. Hailiang Du, Ning Tan, Li Fan et al., *Materials*, **12**, 3097 (2019). htpss://doi.org/10.3390/ma12193097.
11. V.V.Mikhailov, A.E.Gitlevich, A.D.Verkhoturov, *Surf. Eng. Appl. Elect.*, **49**, 373 (2013). htpss://doi.org/10.3103/S1068375513050074
12. A.D.Verkhoturov, I.A.Podchernyaeva, L.F.Pryadko et al., Electrode Materials for Electrospark Alloying, Nauka, Moscow (1988) [in Russian].
13. A.D.Verkhoturov, S.V.Nikolenko, *Strength. Technol. Coat.*, **2**, 13 (2010).
14. A.D.Verkhoturov, V.I.Ivanov, L.A.Konevtsov, *Surf. Eng. Appl. Elect.*, **55**, 241 (2019). htpss://doi.org/10.3103/S106837551903016 5.
15. O.O.Vasiliev, V.B.Muratov, T.I.Duda, *Fizika i Khimiya Tverdogo Tila*, **18**, 358 (2017).
16. P.S.Kisly, V.A.Neronov, T.A.Prikhna et al., Aluminum Borides, Naukova Dumka, Kiev (1990).
17. T.A.Prikhna, P.P.Barvitskyi, M.V.Karpets et al., *J. Superhard Mater.*, **39**, 299 (2017). htpss://doi.org/10.3103/S106345761705001X.
18. UA Patent 107259 (2016).
19. G.N.Dulnev, Yu.P.Zarichnyak, Thermal Conductivity of Mixtures and Composite Materials, Energiya, Leningrad (1974) [in Russian].
20. L.S.Palatnik, *Dokl. Acad. Nauk SSSR*, **LXXXIX**, 455 (1953).
21. O.S.Manakova, A.E.Kudryashov, E.A.Levashov, *Surf. Eng. Appl. Elect.*, **51**, 413 (2015). htpss://doi.org/10.3103/S1068375515050117
22. metallicheckiy-portal.ru/marki_metallov/tit/VT1-0
23. V.I.Ivanov, A.D.Verkhoturov, L.A.Konevtsov, *Surf. Eng. Appl. Elect.*, **53**, 218 (2017). htpss://doi.org/10.3103/S1068375517030061
24. V.S.Kovalenko, A.D.Verkhoturov, L.F.Golovko et al., Laser and Electroerosion Hardening of Materials, Nauka, Moscow (1986) [in Russian].
25. T.Atoda, I.Higashi, M.Kobayashi, *Sci. Pap. Inst. Phys. Chem. Res.*, **61**, 92 (1967).
26. M.Sadhasivam, N.Mohan, S.R.Sankaranarayanan et al., *Mater. Res. Express.*, **7**, 016545 (2020). htpss://doi.org/10.1088/2053-1591/ab6488.
27. R.G.Munro, *J. Res. Natl. Inst. Stan.*, **105**, 709 (2000). doi.org/10.6028/jres.105.057
28. S.A.Pyachin, T.B.Ershova, A.A.Burkov et al., *Russ. J. Non-Ferr. Met.*, **57**, 266 (2016). htpss://doi.org/10.3103/S106782121603013 5.
29. Shao-Guang Liu, Jin-Ming Wu, Sheng-Cai Zhang et al., *Wear*, **262**, 555 (2007). htpss://doi.org/10.1016/j.wear.2006.06.021.
30. Yang Liu, Wensheng Liu, Yunzhu Ma et al., *Surf. Coat. Technol.*, **353**, 32 (2018). htpss://doi.org/10.1016/j.surfcoat.2018.08.067.